Food Chemistry: X 26 (2025) 102288

Contents lists available at ScienceDirect

Food Chemistry: X

journal homepage: www.sciencedirect.com/journal/food-chemistry-x

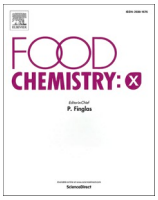

Integrative metabolomics and molecular networking reveal metabolic rewiring in Tartary buckwheat sprouts under moderate hydrostatic pressure

Liangyu Zhang [a], Shuangyong Ding [a], Rui Xu [b], Li Xiao [a], Jianxiong Chen [c], Tao Wu [a,*], Weili Li [a,*]

[a] Food Microbiology Key Laboratory of Sichuan Province, Chongqing Key Laboratory of Speciality Food Co-Built by Sichuan and Chongqing, Xihua University, No.999 Guangchang Road, Chengdu 610039, China.
[b] College of Food Science and Technology, Hebei Normal University of Science and Technology, Qinhuangdao, China.
[c] Sichuan Huan Tai Biotechnology Co., Ltd., 979 Konggang 3rd Road, Shuangliu District, Chengdu, Sichuan Province, Chengdu 610000, China.

ARTICLE INFO

Keywords:
Fagopyrum tataricum
Germination
Feature-based molecular network
Moderate -hydrostatic pressure
UHPLC-Q-TOF-MS/MS

ABSTRACT

The effects of moderate hydrostatic pressure (MHP) pretreatment on bioactive metabolites in *Tartary buckwheat* sprouts remain insufficiently studied. In this work, a non-targeted metabolomics approach, combined with feature-based molecular networking (FBMN), identified 22 metabolites in sprouts treated with 0–30 MPa pressure, four of which were previously unreported, thus expanding the species' phytochemical diversity. MHP treatment activated phenylalanine ammonia-lyase (PAL), resulting in a 2.3-fold increase in total flavonoids, particularly glycosylated derivatives such as quercetin 3-rutinoside 7-glucoside (13.2-fold increase at 25 MPa). In contrast, condensed tannins, responsible for astringency, were reduced by 40–60 %. These findings suggest that MHP pretreatment may serve as a sustainable alternative to chemical elicitors, promoting biofortification and improving sensory attributes in sprout-based functional foods.

1. Introduction

Tartary buckwheat (*Fagopyrum tataricum* Gaertn.), a nutrient-dense pseudocereal of the Polygonaceae family, has become a strategic crop in Asian high-altitude agriculture, particularly throughout the Himalayan regions encompassing China, India, Nepal, and Bhutan. Its exceptional agronomic resilience enables cultivation in marginal soils under extreme climatic conditions, a trait attributed to sophisticated stress-response mechanisms (Luthar et al., 2021). Phytochemical profiling reveals extraordinary concentrations of C-glycosyl flavonoids, particularly rutin, with groats containing 81.3 ± 2.1 mg/g dry weight — 478 % higher than common buckwheat (*F. esculentum* Moench) (Kreft et al., 2023). While these flavonoids impart characteristic bitter notes, their demonstrated bioactivity as radical scavengers, inflammation modulators, and vascular protector's positions Tartary buckwheat as a prime candidate for nutraceutical innovation (Dong et al., 2023).

Emerging bioprocessing strategies, particularly controlled sprouting, have shown remarkable potential for amplifying the bioavailability of bioactive constituents in cereal matrices, including phenolic acids, γ-aminobutyric acid (GABA), and soluble dietary fibers (Kaur et al., 2024). Recent advances in physical modulation techniques reveal that moderate hydrostatic pressure (MHP; 10–100 MPa) can precisely orchestrate enzymatic activation in germinating seeds. For instance, short-term MHP exposure (30–90 MPa, 5 min) enhanced GABA synthesis in brown rice sprouts by 2.8-fold through allosteric regulation of glutamate decarboxylase (EC 4.1.1.15) (Q. Xia & Li, 2018a). However, current research remains disproportionately focused on true cereals, with critical knowledge gaps persisting regarding: (1) pressure-induced metabolic reprogramming in pseudocereals, and (2) the molecular interplay between mechanical stress signaling and secondary metabolite biosynthesis during pseudocereal germination. Elucidating these mechanisms represents an essential step toward engineering functionally enhanced sprouted ingredients for the global health food sector.

Ultra-high-performance liquid chromatography coupled with quadrupole time-of-flight mass spectrometry (UHPLC-Q-TOF-MS)-based untargeted metabolomics has emerged as a critical tool for investigating stress-induced metabolic shifts in plant systems.

State-of-the-art metabolomic platforms, particularly ultra-high-performance liquid chromatography coupled with quadrupole time-of-flight mass spectrometry (UHPLC-Q-TOF-MS), deliver ppm-level mass

* Corresponding authors:
E-mail addresses: wutaobox@gmail.com (T. Wu), liweili1207@126.com (W. Li).

https://doi.org/10.1016/j.fochx.2025.102288
Received 16 September 2024; Received in revised form 2 February 2025; Accepted 15 February 2025
Available online 17 February 2025
2590-1575/© 2025 The Authors. Published by Elsevier Ltd. This is an open access article under the CC BY-NC-ND license (http://creativecommons.org/licenses/by-nc-nd/4.0/).

accuracy, enabling comprehensive resolution of stress-responsive metabolic networks (Y. Wang et al., 2024). Nevertheless, conventional spectral library matching approaches exhibit significant limitations in characterizing metabolites, primarily due to inadequate reference spectral coverage. To address this, the Global Natural Products Social Molecular Networking (GNPS) platform combined with Feature-Based Molecular Networking (FBMN) implements a multi-tiered analytical strategy: (i) MS/MS spectral networking based on modified cosine similarity scoring (threshold >0.7), (ii) computational dereplication using NPClassifier algorithms, and (iii) annotated substructure propagation through molecular family networks (Caldas et al., 2022; Mei et al., 2024). This integrated approach facilitates de novo structural elucidation of both biosynthetic intermediates and stress-specific biomarkers.

This study endeavors to clarify the mechanisms behind MHP-induced metabolic reprogramming in Tartary buckwheat sprouts. By integrating untargeted metabolomics with FBMN analysis, we aim to identify the key metabolites and biochemical pathways affected by MHP treatment. This effort will lay the groundwork for optimizing germination strategies and enhancing the functional value of pseudocereal sprouts.

2. Materials and methods

2.1. Samples and reagents

Tartary buckwheat seeds were procured from Sichuan Huan Tai Biological Technology Co., Ltd. Formic acid, methanol, and acetonitrile were purchased from Sigma-Aldrich (Shanghai, China). Ultra-pure water (18.2 MΩ·cm) was obtained using a Milli-Q system (Millipore, Bedford, MA, USA).

2.2. Sample preparation

The sample preparation was based on the moderate -pressure treatment method developed by Xia et al. (Q. Xia & Li, 2018b). Tartary buckwheat seeds (100 g) were weighed and placed in a sealed bag, and 10 mL of deionized water was added before vacuum sealing. The seeds were then divided into a control group (0 MPa) and a pressure treatment group (20, 25, and 30 MPa). The samples in the pressure-treatment groups were subjected to moderate -pressure processing for 5 min using specialized equipment. Subsequently, the seeds from each group were immersed in 20 mL of 1 % sodium hypochlorite solution for 10 min, followed by rinsing with deionized water until neutral PH was achieved. The soaked Tartary buckwheat seeds were placed in a constant temperature incubator at 25 °C for 48 h for germination and watered every 8 h to maintain the moisture of the seed surface. After germination, the seeds were dried in a constant-temperature drying oven at 50 °C for hot-air drying. Once the seeds had dried, they were ground into a fine powder using an ultrafine pulverizer, sifted through an 80-mesh sieve, and stored at −20 °C for later use.

2.3. Sample extraction

1.0 g of tartary buckwheat powder was accurately weighed into a 15 mL polypropylene centrifuge tube. A 10 mL aliquot of a 50 % (*v*/v) methanol aqueous solution was added, followed by homogenization using a vortex mixer at 3000 rpm for 3 min. Ultrasonic-assisted extraction was then performed in a temperature-controlled ultrasonic bath (40 kHz, 25 ± 2 °C) for 20 min. The mixture was centrifuged at 2500 ×*g* for 15 min at 4 °C to separate the solid residue. The supernatant was collected and filtered through a 0.25 μm PTFE syringe filter (Millipore, USA) to obtain a particle-free extract, which was stored at −20 °C pending chromatographic analysis.

2.4. UHPLC-Q-TOF-MS analysis

UHPLC-Q-TOF-MS analysis was conducted using a Shim-pack ODS III column (Shimadzu, Tokyo, Japan; 2.1 mm × 100 mm, 1.6 μm particle size). The mobile phase consisted of acetonitrile (solvent B) and 0.1 % (*v*/v) formic acid aqueous solution (solvent A), with gradient elution performed at a flow rate of 0.25 mL/min. The elution gradient was programmed as follows: 0–1 min, 10 % B; 1–6 min, 10–30 % B; 6–12 min, 30–50 % B; 12–14 min, 70–85 % B; 16–17 min, 85–90 % B; 17–22 min, 90–100 % B; 23–25 min, 100–10 % B; 25–27 min, 10 % B. The injection volume was set at 2.0 μL, and the column temperature was maintained at 40 °C.

Mass spectrometric analysis was performed using a SCIEX X500R (SCIEX, USA, CA) in negative ion mode, equipped with an electrospray ionization (ESI) source. Data acquisition was conducted in information-dependent acquisition (IDA) mode, collecting ions within the *m/z* range of 100–1000 Da. The MS^1 collision energy (CE) was set at −10 V, with a fragment ion scan accumulation time of 0.08 s per spectrum. For MS^2 acquisition, the MS^2 CE was set at −25 V ± 15 V, and the top 10 most intense ions were selected for fragmentation in each acquisition cycle.

2.5. Evaluation of phenylalanine Ammonia-Lyase (PAL) activity

Freeze-dried Tartary buckwheat powder (2 g) was homogenized in 5 mL ice-cold potassium borate buffer (pH 8.8, 2 mM mercaptoethanol), vortexed, and centrifuged at 4500 rpm, 4 °C, for 15 min. The supernatant was collected as the enzyme extract. The activity of PAL was determined by measuring the content of cinnamic acid formed.

A reaction mixture containing 0.1 mL enzyme extract, 1.1 mL potassium borate buffer (pH 8.8), and 0.8 mL 3 mM *L*-phenylalanine was incubated at 37 °C for 1 h. The reaction was terminated with 0.1 mL 6 M HCl, followed by extraction of cinnamic acid with 15 mL ethyl acetate. The organic phase was evaporated at 80 °C and redissolved in methanol for analysis.

Cinnamic acid concentration was determined using a standard curve (0–50 μg/mL) with absorbance measured at 290 nm. The regression equation was:

Y= 0.08818 + 0.11806 X ($R = 0.998$) where Y is absorbance and X is cinnamic acid concentration (μg/mL).

2.6. Molecular network analysis

Raw UHPLC-Q-TOF-MS data were preprocessed in MS-DIAL v4.90 (RIKEN, Japan). Processed .mgf files were submitted to the Global Natural Products Social Molecular Networking (GNPS) platform (https://gnps.ucsd.edu/) for feature-based molecular networking (FBMN) with the default parameters default settings: cosine score > 0.7, minimum matched peaks = 5, and maximum precursor mass difference = 0.02 Da. Resulting networks were imported into Cytoscape 3.9.1 (National Institute of General Medical Sciences, USA) with node sizes scaled to MS1 peak intensities (Nothias et al., 2020). (Otasek et al., 2019).

2.7. Multivariate statistical analysis

LC-MS feature tables were Pareto-scaled and log-transformed prior to multivariate analysis. Principal component analysis (PCA) and orthogonal partial least squares discriminant analysis (OPLS-DA) were executed via MetaboAnalyst 5.0 (https://www.metaboanalyst.ca/). Differentially abundant metabolites (fold change greater than 2 or less than 0.5 and $P < 0.05$ by permutation test) were hierarchically clustered (Euclidean distance, Ward's linkage) using OmicStudio (https://www.omicstudio.cn/) to generate heatmaps annotated with Kyoto Encyclopedia of Genes and Genomes (KEGG) pathway classifications.

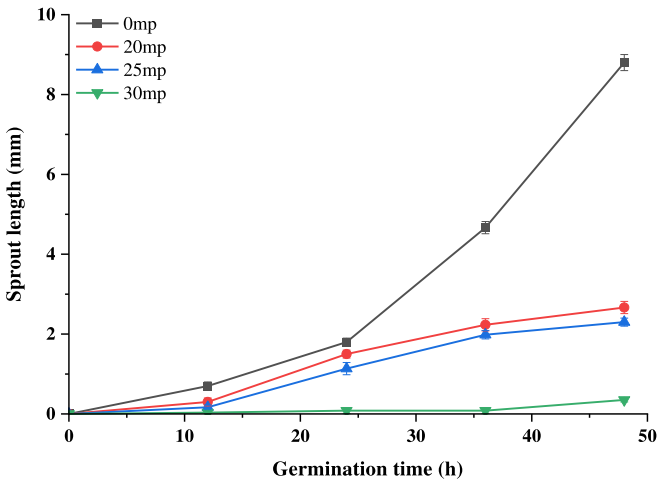

Fig. 1. Effects of moderate hydrostatic pressure (MHP) pretreatment on sprout length in germinated *Fagopyrum tataricum* seeds. Seeds were subjected to 0, 20, 25, and 30 MPa pressure ($n = 3$).

3. Results

3.1. Impact of MHP processing on sprout elongation in Tartary buckwheat

MHP pretreatment significantly suppressed sprout elongation in Tartary buckwheat during the 48-h germination period (Fig. 1). While control seeds (0 MPa) exhibited progressive growth, reaching 9 mm by the endpoint, MHP-treated seeds (20–30 MPa) showed dose-dependent inhibition, with final sprout lengths reduced to 0.2–2 mm. The strongest suppression occurred at 30 MPa, achieving over 95 % inhibition compared to controls. This suggests that MHP disrupts critical germination processes, including cell division, enzymatic activity, and water absorption.

The 20–30 MPa range was prioritized for its ability to modulate germination without complete suppression, consistent with prior reports linking this pressure range to stress-induced bioactive compound accumulation in seeds. Notably, analogous MHP treatments enhanced γ-aminobutyric acid (GABA) levels in brown rice (Xia & Li, 2018a) and upregulated flavonoid biosynthesis in buckwheat sprouts (Ruan et al., 2021), supporting our rationale for selecting this pressure range to balance metabolic stimulation with viability retention.

3.2. Metabolic profiling and molecular network characterization

To systematically characterize the pressure-induced modulation of secondary metabolism in germinating Tartary buckwheat, we implemented an integrated analytical workflow combining untargeted metabolomics with FBMN. Sprouts from four MHP treatment groups (0, 20, 25, and 30 MPa) were profiled using UHPLC-Q-TOF-MS/MS to resolve metabolic perturbations underlying their phytochemical composition.

The FBMN analysis of MS^2 spectral data (4000 feature ions, including $[M\text{-}H]^-$ and $[M + FA\text{-}H]^-$ adducts) revealed 23 molecular families (networks ≥2 nodes), enabling structural annotation through GNPS spectral library matching (Fig. 2A). Cross-validation with the MS-DIAL database confirmed 22 annotated metabolites, with chromatographic parameters (retention time), accurate mass measurements (*m/z*), and classification details systematically documented in Table 1. The identified compounds predominantly belonged to anthraquinones and flavonoids, including four novel reports in Tartary buckwheat: quercetin-3′-glucoside, endocrocin, quercetin trimer, and uralenol. These findings significantly expand current understanding of this species' specialized metabolic repertoire.

3.2.1. Structural elucidation of flavonoids

FBMN demonstrated superior structural resolution compared to conventional database matching by utilizing intra-family relationships to deduce unknown compound architectures. In the flavonoid molecular family (M1, Fig. 2), compounds B and E were identified as quercimeritrin and quercetin dimers, respectively, through spectral matching with existing databases. The structures of compounds C, D, and F were further elucidated based on their MS/MS fragmentation patterns. Adduct ion analysis provided additional structural evidence: compounds C ($[M + FA\text{-}H]^-$ *m/z* 625.1474) showed diagnostic adduct patterns confirming their parent ion masses.

Flavonoids typically undergo a distinct fragmentation process known as Retro-Diels-Alder (RDA) cleavage (van Dinteren et al., 2021). For example, quercetin exhibits characteristic ion fragments, such as *m/z* 151 in its MS/MS spectrum, indicative of cleavage at positions C1 and C3 of the C-ring (Fig. 5B) (W. Li, Zhou, et al., 2023).

Compound C exhibited a molecular ion at m/z 625.1474, along with typical flavonoid aglycone fragments at m/z 463.0910 and m/z 301.0380. Based on literature data, compound C was inferred to undergo the loss of a glucose moiety at the 3rd position, leading to its preliminary identification as quercetin 3,7-diglucoside (Park et al., 2024).

Compound D demonstrated a fragmentation profile analogous to compound B, featuring signature ions at *m/z* 301.0350, 178.9990, 151.0040, and 121.0290. The 94.0680 Da mass difference (ΔCH_2O_5) from compound B supported its identification as uralenol (A. Wang et al., 2018). Similarly, compound E's quercetin-like fragmentation pattern (*m/z* 301.0360, 178.9990, 151.0040) confirmed its dimeric nature. The 302.0940 Da mass difference between compounds E and F suggested sequential quercetin unit loss, indicating compound F's trimeric configuration.

3.2.2. Anthraquinone structural characterization

The anthraquinone molecular family (M2, Fig. 2) contained several structurally related compounds. Database matching confirmed emodin (H) identification, while FBMN analysis facilitated endocrocin (G) annotation. Compound G displayed a 44 Da mass reduction compared to emodin (ΔCO_2), consistent with anthraquinone decarboxylation patterns. This characteristic mass shift, combined with spectral data, supported compound G's identification as endocrocin (Christiansen et al., 2022).

3.3. PCA analysis

Principal Component Analysis (PCA) is a widely used technique for reducing data complexity by consolidating multiple interrelated variables into a smaller set of comprehensive indicators. As shown in Fig. 3A, the metabolite profiles of the moderate -pressure treatment groups (20, 25, and 30 MPa) exhibited clear separation from the control group (0 MPa), highlighting substantial metabolic alterations induced by moderate hydrostatic pressure (MHP). The inclusion of all samples within the 95 % confidence interval reinforces the robustness of the analysis. Notably, the first two principal components, PC1 and PC2, accounted for 70.3 % and 18.8 % of the variance, respectively, collectively explaining 89.1 % of the total variance, underscoring the strong discriminatory power of the measured variables.

The PCA plot further illustrates the directional shifts in metabolite composition under different pressure conditions. Specifically, the control group (red) clustered primarily in the bottom-left quadrant, while moderate -pressure groups (green, light blue, and dark blue) shifted progressively rightward along the PC1 axis, indicating pressure-induced metabolic adaptations. While changes along the PC2 axis were less pronounced, they still suggest biologically relevant variations in secondary metabolic pathways. These results collectively indicate that MHP treatment significantly influences metabolic pathways, potentially promoting the synthesis of bioactive compounds in Tartary buckwheat

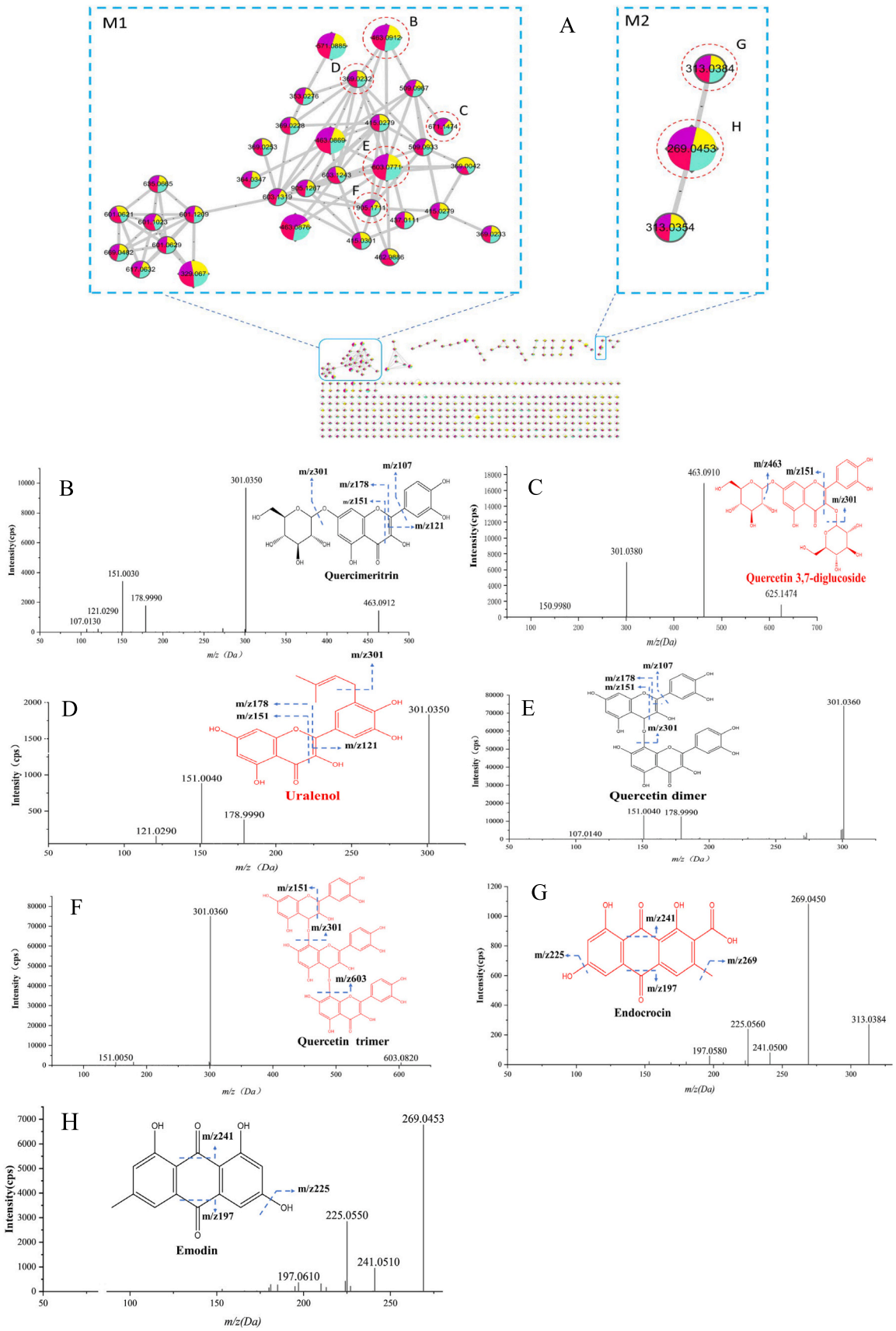

Fig. 2. (A) Feature-Based Molecular Networking (FBMN) analysis of mass spectrometry data to identify molecular families. MS/MS fragmentation patterns of (B) quercimeritrin, (C) quercetin 3,7-diglucoside, (D) uralenol, (E) quercetin dimer, (F) quercetin trimer, (G) endocrocin, and (H) emodin.

Table 1
Annotation of 22 metabolites in *Fagopyrum tataricum*.

No.	Rt (min)	*m/z* (Da)	Adduct	Name	Classification
1	12.22	269.0453	[M-H]⁻	Emodin	Anthraquinones
2	7.36	273.0768	[M-H]⁻	Phloretin	Chalcones and dihydrochalcones
3	7.61	285.0405	[M-H]⁻	Kaempferol	Flavones
4	2.85	289.0718	[M-H]⁻	Catechin	Flavans
5	6.68	301.0354	[M-H]⁻	Quercetin	Flavones
6	5.07	303.0510	[M-H]⁻	Taxifolin	Flavans
7	8.41	313.0384	[M-H]⁻	Endocrocin	Anthracenecarboxylic acids and derivatives
8	7.80	315.0510	[M-H]⁻	Isorhamnetin	Flavones
9	8.11	329.0667	[M-H]⁻	Quercetin 3,7-dimethyl ether	*O*-methylated flavonoids
10	1.44	369.0232	[M-H]⁻	Uralenol	Flavones
11	1.34	431.0984	[M-H]⁻	Vitexin	Flavonoid glycosides
12	5.23	447.0933	[M-H]⁻	Astragalin	Flavonoid glycosides
13	5.23	447.0933	[M-H]⁻	Kaempferol-7-O-glucoside	Flavonoid glycosides
14	4.53	463.0882	[M-H]⁻	Spiraeoside	Flavonoid glycosides
15	5.29	463.0912	[M-H]⁻	Quercimeritrin	Flavonoid glycosides
16	2.35	577.1351	[M-H]⁻	Procyanidin B2	Biflavonoids and polyflavonoids
17	6.67	603.0780	[2 M-H]⁻	Quercetin dimer	Flavonolignans
18	5.18	609.1461	[M-H]⁻	Rutin	Flavonoid glycosides
19	3.45	671.1474	[M + FA-H]⁻	Quercetin 3,7-diglucoside	Flavonoid glycosides
20	3.00	771.1989	[M-H]⁻	Quercetin 3-Rutinoside 7-glucoside	Flavonoid glycosides
21	2.85	865.1985	[M-H]⁻	Procyanidin trimer	Biflavonoids and polyflavonoids
22	6.67	905.1207	[3 M-H]⁻	Quercetin trimer	Flavonolignans

sprouts.

In summary, Fig. 3A visually demonstrates how increasing pressure levels drive distinct metabolic responses, reinforcing the role of MHP in modulating plant metabolomics. These findings provide a strong basis for further investigations into the physiological mechanisms underlying plant stress responses.

3.4. PLS-DA analysis

Partial Least Squares Discriminant Analysis (PLS-DA) is a supervised statistical method used to differentiate sample categories by modeling relationships between omics data and sample classification. As illustrated in Fig. 3B, the PLS-DA model achieved a high R^2Y value of 0.987, explaining nearly 99 % of the variance in the Y-direction, which indicates an excellent model fit. Additionally, the Q^2 value reached 0.922, demonstrating strong predictive accuracy for new data, further confirming the robustness of the analysis.

The distinct separation observed in Fig. 3B between the control group and the three moderate -pressure treatment groups emphasize the substantial metabolic shifts induced by MHP. Notably, the clustering pattern within each pressure group was highly compact, indicating high

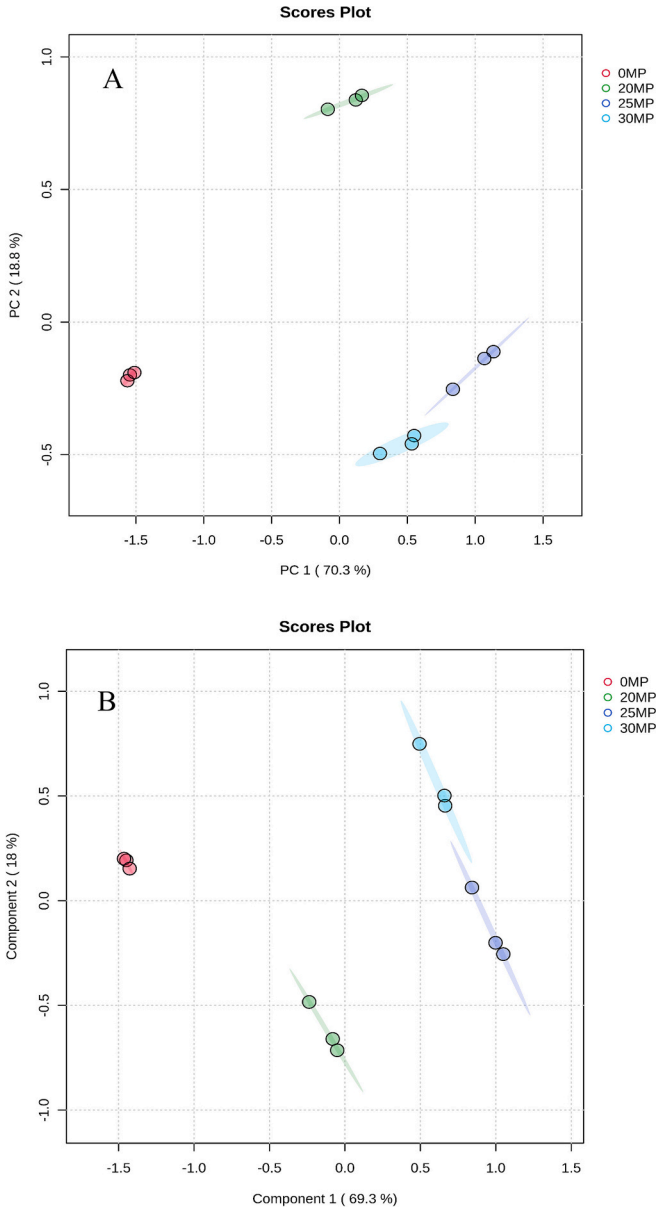

Fig. 3. Multivariate analysis of *Fagopyrum tataricum* sprouts: (A) principal component analysis (PCA) score plot and (B) partial least-squares discriminant analysis (PLS-DA).

intra-group consistency in metabolite variations. This suggests that MHP treatment leads to reproducible metabolic changes, reinforcing its influence on metabolite biosynthesis in Tartary buckwheat sprouts. This result further highlights the potential of multivariate statistical approaches in metabolomics research, particularly for exploring stress-induced biochemical transformations in seeds.

3.5. Differential metabolites under different pressure conditions

The effect of three intensities of pressure on metabolites was analyzed through metabolite differentiation, and significant metabolites were determined based on fold change (greater than 2 or less than 0.5) and $P < 0.05$. As shown in Fig. 4, pressure treatment induced notable metabolic responses, with 12, 10, and 13 differential metabolites identified at 20, 25, and 30 MPa, respectively.

At 20 MPa, 12 flavonoids, including quercimeritrin, emodin, and quercetin 3-rutinoside 7-glucoside, were upregulated by 5.32-fold ($P = 0.003$), 5.18-fold ($P = 0.008$), and 5.05-fold ($P = 0.012$), respectively.

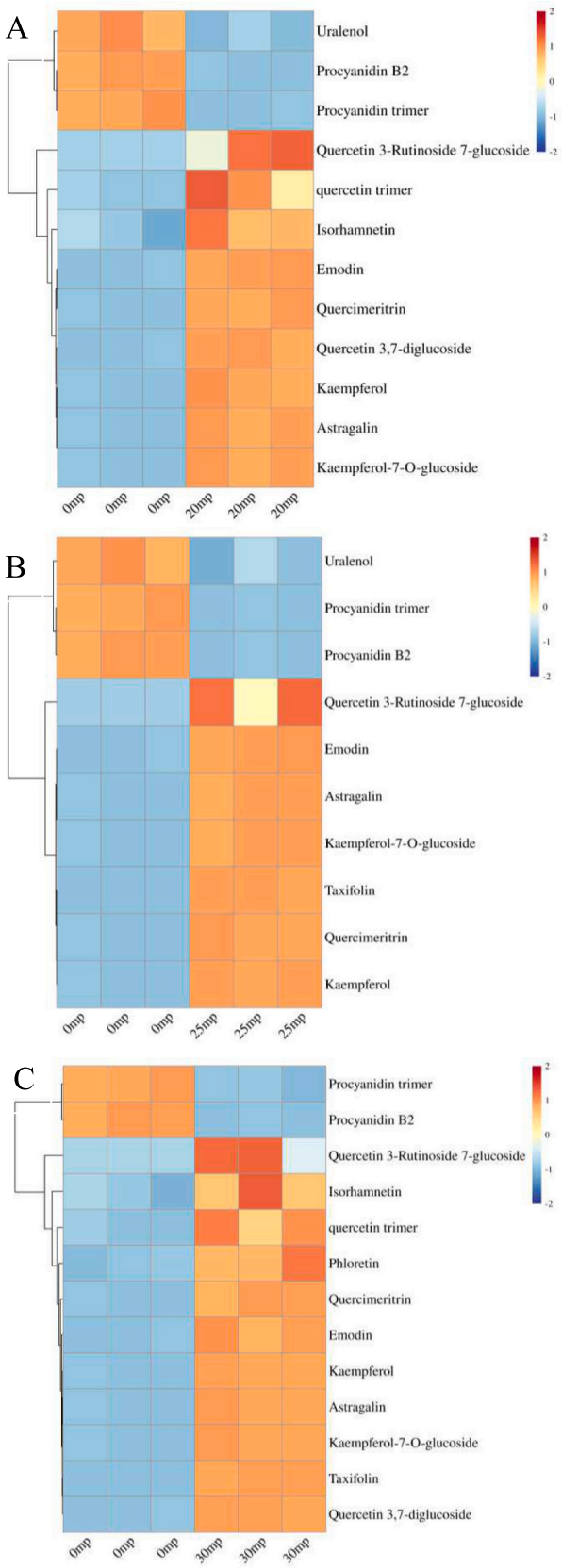

Fig. 4. Heatmap analysis of metabolite profiles in *Fagopyrum tataricum* sprouts under different pressure conditions: (A) 20 MPa, (B) 25 MPa, and (C) 30 MPa.

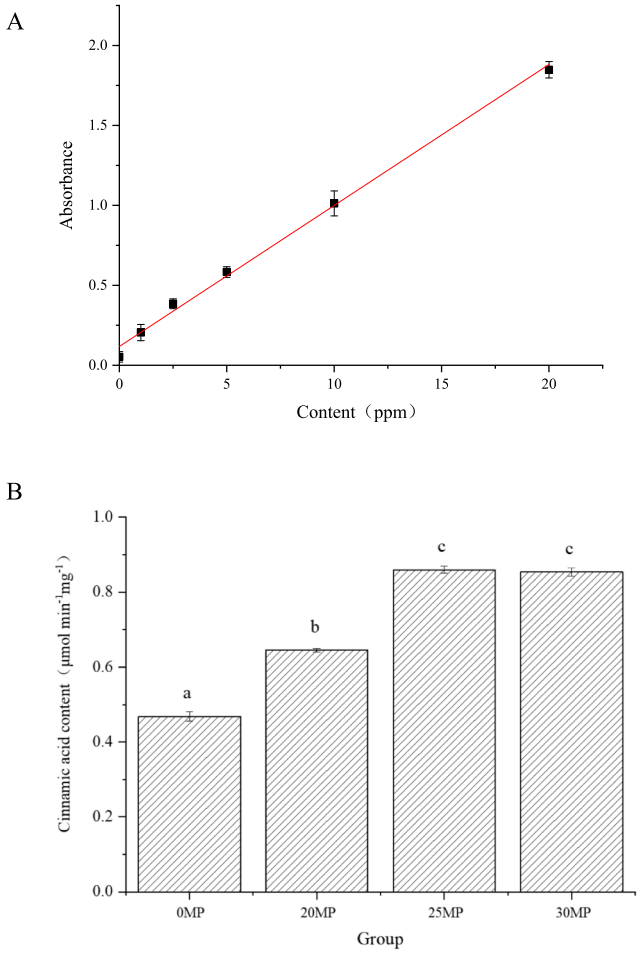

Fig. 5. (A) Standard curve for cinnamic acid quantification. (B) Effects of varying pressure treatments on cinnamic acid content, reflecting phenylalanine ammonia-lyase (PAL) activity in *Fagopyrum tataricum* sprouts.

Additionally, kaempferol and astragalin showed approximately two-fold upregulation. In contrast, procyanidin B2, procyanidin trimer, and uralenol decreased significantly by 4.0-fold, 3.8-fold, and 2.8-fold, respectively, suggesting that anthocyanin-related compounds are sensitive to pressure.

At 25 MPa, 10 metabolites showed significant changes. Taxifolin (FC = 26.4, $P < 0.0001$) and quercetin 3-rutinoside 7-glucoside (FC = 13.2, $P = 0.0003$) increased by 26-fold and 13-fold, respectively. Emodin and quercimeritrin showed slight reductions in upregulation but remained significantly elevated (4.6- and 4.9-fold), while kaempferol, kaempferol-7-O-glucoside, and astragalin continued to show enrichment at levels above two-fold.

At 30 MPa, 13 metabolites were upregulated, including phloretin, kaempferol, quercetin trimer, quercetin 3,7-diglucoside, astragalin, kaempferol-7-O-glucoside, and isorhamnetin, all of which increased by more than two-fold. Quercimeritrin, emodin, and quercetin 3-rutinoside 7-glucoside increased by 4–6-fold, while taxifolin exhibited a dramatic 22-fold increase. These results further emphasize the significant regulation of metabolite accumulation under pressure, with complex dynamics observed.

3.6. Pressure modulation of PAL activity

PAL, a pivotal enzyme in the phenylpropanoid pathway, serves as a critical regulator of plant defense mechanisms and phenolic biosynthesis. In this investigation, we quantitatively assessed PAL activity through spectrophotometric determination of cinnamic acid production,

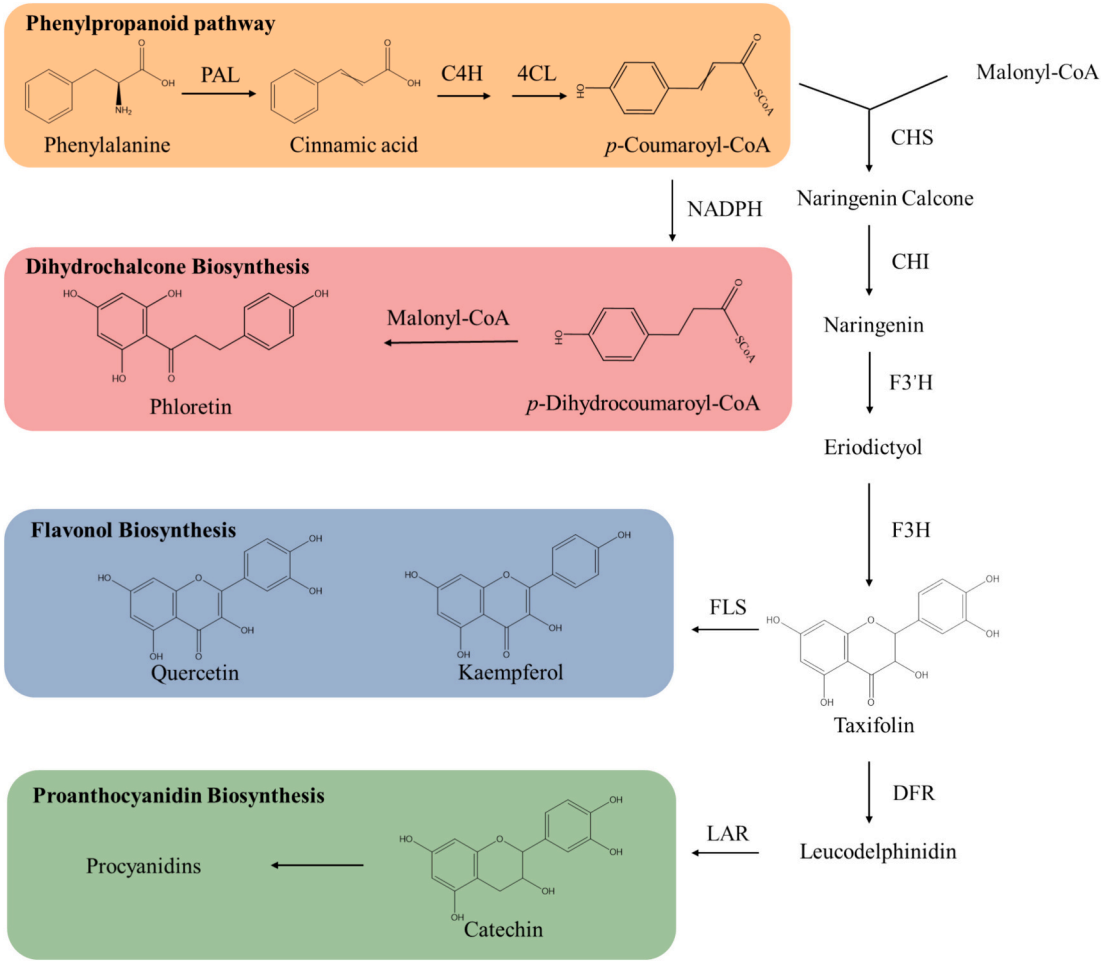

Fig. 6. Schematic representation of high-pressure stress-induced modulation of three key flavonoid biosynthesis pathways in *Fagopyrum tataricum* sprouts.

the enzymatic product of *L*-phenylalanine deamination. Method validation established excellent linearity ($R = 0.998$) in the cinnamic acid standard curve (Fig. 5A), with the derived linear regression eq. ($Y = 0.08818 + 0.11806\times$) providing a reliable quantitative framework for enzymatic activity determination.

Pressure-dependent modulation of secondary metabolite biosynthesis was evaluated through cinnamic acid quantification across varying hydrostatic pressures. Baseline measurements at atmospheric pressure (0 MPa) revealed minimal cinnamic acid accumulation (0.46 mg/g DW) (Fig. 5B). Pressure elevation to 20 MPa significantly enhanced cinnamic acid production to 0.64 mg/g DW, demonstrating pressure-induced activation of PAL-mediated phenylpropanoid metabolism. This stimulatory effect intensified at 25 MPa, with cinnamic acid levels reaching 0.85 mg/g DW, indicating sustained pathway activation under moderate pressure conditions.

Contrastingly, at 30 MPa, we observed a marginal reduction in cinnamic acid accumulation (0.82 mg/g DW), potentially reflecting stress-induced metabolic constraints where supraphysiological pressures may compromise enzymatic efficiency. Statistical analysis revealed no significant difference in PAL activity between 25 MPa and 30 MPa (Fig. 5), suggesting remarkable enzymatic resilience under elevated pressure conditions. This pressure-dependent modulation pattern indicates an optimal pressure range (20–25 MPa) for PAL activation in Tartary buckwheat sprouts, beyond which enzymatic efficiency may plateau or slightly decline.

4. Discussion

The present investigation establishes MHP (20–30 MPa) as a precision biophysical tool for metabolic engineering in Tartary buckwheat sprouts, uniquely enhancing bioactive compound biosynthesis while enhancing sensory quality. Our integrated metabolomics and FBMN approach resolved 22 pressure-responsive metabolites, including four previously unreported compounds in this species: quercetin-3′-glucoside, endocrocin, quercetin trimer, and uralenol. These findings substantially expand the known phytochemical repertoire of Tartary buckwheat while revealing MHP's capacity to direct metabolic flux toward nutraceutically valuable pathways, contrasting with the indiscriminate stress responses elicited by conventional abiotic triggers like drought or UV exposure (Dixon & Sarnala, 2020).

Central to this metabolic reprogramming is the pressure-sensitive modulation of phenylpropanoid metabolism, governed by PAL dynamics. The biphasic PAL activity profile—peaking at 25 MPa (0.85 mg/g DW cinnamic acid) with sustained functionality at 30 MPa—drives a 2.3-fold flavonoid accumulation through enhanced chalcone synthase activity (Fig. 6). Notably, MHP preferentially enriches flavonoid glycosides (e.g., quercetin 3-rutinoside 7-glucoside, 13.2-fold at 25 MPa) while suppressing condensed tannins (40–60 % reduction in procyanidin B2 and catechin), a metabolic partitioning pattern distinct from jasmonate-induced responses that broadly activate competing pathways (Zhang et al., 2024). This selective inhibition of dihydroflavonol reductase (DFR) redirects substrates toward glycosylation, yielding metabolites with enhanced bioavailability and sensory compatibility—quercetin trimer (4.6-fold) and isorhamnetin (2.8-fold) exemplify

this trend, their cardioprotective and antioxidant properties being well-documented (Mirza et al., 2023; S. Xia et al., 2019). Concurrent reduction of astringent procyanidins addresses a key sensory barrier in sprout utilization (Osakabe et al., 2024), positioning MHP as a dual-purpose technology for nutraceutical and palatability enhancement.

The divergent pressure responses observed between flavonoid and anthraquinone biosynthesis pathways highlight opportunities for process optimization in Tartary buckwheat sprouts. While key anthraquinones such as emodin and endocrocin exhibited moderate induction (4–6-fold), their accumulation plateaued at 30 MPa, contrasting with the sustained upregulation of flavonoids. This discrepancy may reflect redox limitations or differential enzymatic regulation in anthraquinone biosynthesis under high-pressure conditions. Such pathway-specific modulation underscores the precision of moderate hydrostatic pressure (MHP) as a biophysical tool, enabling targeted enrichment of bioactive phytochemicals without the collateral metabolic trade-offs often associated with chemical elicitors.

To further elucidate the biological significance of these findings, future research should integrate transcriptomic and proteomic analyses to unravel the molecular mechanisms underlying pressure sensing and signal transduction in Tartary buckwheat sprouts. Investigating the roles of key regulatory enzymes, redox-sensitive transcription factors, and mechanical stress-responsive genes will provide deeper insights into the metabolic reprogramming induced by MHP.

5. Conclusion

This study shows that MHP (20–30 MPa) precisely modulates the specialized metabolism in Tartary buckwheat sprouts. It selectively boosts bioactive flavonoids and anthraquinones while suppressing unwanted tannins. The pressure-dependent activation of PAL forms a mechanistic link between mechanical stress and phenylpropanoid flux, resulting in a 2.3-fold enrichment of flavonoids, mainly glycosylated derivatives with enhanced bioactivity. By avoiding the sensory issues and metabolic redundancy of conventional elicitors, MHP becomes a sustainable option for functional ingredient engineering.

However, for practical food industry applications, several challenges need to be tackled along with actionable solutions. The high energy demand of MHP systems, which restricts scalability, is a major hurdle. Integrating energy-efficient technologies like regenerative pressure recovery systems can cut operational costs by 30–40 % to mitigate this. Moreover, optimizing pressure-time parameters for large-scale hydroponic systems can improve energy efficiency while maintaining metabolite consistency. By overcoming these translational barriers, MHP can transform from a laboratory innovation into a scalable tool for sustainable nutraceutical production, meeting the global food industry's need for precision biofortification technologies.

Abbreviations

PAL	phenylalanine ammonia lyase
C4H	cinnamic acid 4-hydroxylase
4CL	4-coumarate-CoA ligase
CHS	chalcone synthase
CHI	chalcone isomerase
F3'H	flavanone 3′-hydroxylase
F3H	flavanone 3-dioxygenase
FLS	flavonol synthase
DFR	dihydroflavonol 4-reductase
LAR	leucoanthocyanidin reductase.

CRediT authorship contribution statement

Liangyu Zhang: Writing – original draft. **Shuangyong Ding:** Validation. **Rui Xu:** Methodology. **Li Xiao:** Methodology. **Jianxiong Chen:** Investigation. **Tao Wu:** Writing – review & editing, Supervision, Conceptualization. **Weili Li:** Supervision, Methodology.

Declaration of competing interest

The authors declare that they have no known competing financial interests or personal relationships that could have appeared to influence the work reported in this paper.

Acknowledgments

We are grateful for the financial support from Xihua Program, China (D202405311434206590).

Data availability

Data will be made available on request.

References

Caldas, L. A., Zied, D. C., & Sartorelli, P. (2022). Dereplication of extracts from nutraceutical mushrooms Pleurotus using molecular network approach. *Food Chemistry, 370*, Article 131019. https://doi.org/10.1016/j.foodchem.2021.131019

Christiansen, J. V., Larsen, T. O., & Frisvad, J. C. (2022). Production of fungal Quinones: Problems and prospects. *Biomolecules, 12*(8), 1041. https://doi.org/10.3390/biom12081041

Dixon, R. A., & Sarnala, S. (2020). Proanthocyanidin biosynthesis—A matter of protection. *Plant Physiology, 184*(2), 579–591. https://doi.org/10.1104/pp.20.00973

Dong, Y., Wang, N., Wang, S., Wang, J., & Peng, W. (2023). A review: The nutrition components, active substances and flavonoid accumulation of Tartary buckwheat sprouts and innovative physical technology for seeds germinating. *Frontiers in Nutrition, 10*. https://doi.org/10.3389/fnut.2023.1168361

Kaur, N., Gasparre, N., & Rosell, C. M. (2024). Expanding the application of germinated wheat by examining the impact of varying alpha-amylase levels from grain to bread. *Journal of Cereal Science, 120*, Article 104059. https://doi.org/10.1016/j.jcs.2024.104059

Kreft, I., Golob, A., & Germ, M. (2023). A crop of high nutritional quality and health maintenance value: The importance of Tartary buckwheat breeding. *Agriculture, 13*(9), 1783. https://doi.org/10.3390/agriculture13091783

Luthar, Z., Golob, A., Germ, M., Vombergar, B., & Kreft, I. (2021). Tartary buckwheat in human nutrition. *Plants, 10*(4), 700. https://doi.org/10.3390/plants10040700

Mei, S., Yao, S., Mo, J., Wang, Y., Tang, J., Li, W., & Wu, T. (2024). Integration of cloud-based molecular networking and docking for enhanced umami peptide screening from Pixian douban. *Food Chemistry: X, 21*, Article 101098. https://doi.org/10.1016/j.fochx.2023.101098

Mirza, M. A., Mahmood, S., Hilles, A. R., Ali, A., Khan, M. Z., Zaidi, S. A. A., … Ge, Y. (2023). Quercetin as a therapeutic product: Evaluation of its pharmacological action and clinical applications—A review. *Pharmaceuticals, 16*(11), 1631. https://doi.org/10.3390/ph16111631

Osakabe, N., Fushimi, T., Fujii, Y., & Calabrese, V. (2024). Procyanidins and sensory nutrition; do procyanidins modulate homeostasis via astringent taste receptors? *Bioscience, Biotechnology, and Biochemistry, 88*(4), 361–367. https://doi.org/10.1093/bbb/zbad154

Otasek, D., Morris, J. H., Bouças, J., Pico, A. R., & Demchak, B. (2019). Cytoscape automation: Empowering workflow-based network analysis. *Genome Biology, 20*(1), 185. https://doi.org/10.1186/s13059-019-1758-4

Wang, A., Lu, Y., Du, X., Shi, P., & Zhang, H. (2018). A theoretical study on the antioxidant activity of Uralenol and Neouralenol scavenging two radicals. *Structural Chemistry, 29*(4), 1067–1075. https://doi.org/10.1007/s11224-018-1090-8

Wang, Y., Ma, C., Yang, Y., Wang, B., Liu, X., Wang, Y., Bian, X., Zhang, G., & Zhang, N. (2024). Effect of high hydrostatic pressure treatment on food composition and applications in food industry: A review. *Food Research International, 195*, Article 114991. https://doi.org/10.1016/j.foodres.2024.114991

Xia, Q., & Li, Y. (2018a). Mild high hydrostatic pressure pretreatments applied before soaking process to modulate wholegrain brown rice germination: An examination on embryo growth and physicochemical properties. *Food Research International, 106*, 817–824. https://doi.org/10.1016/j.foodres.2018.01.052

Xia, Q., & Li, Y. (2018b). Mild high hydrostatic pressure pretreatments applied before soaking process to modulate wholegrain brown rice germination: An examination on embryo growth and physicochemical properties. *Food Research International, 106*, 817–824. https://doi.org/10.1016/j.foodres.2018.01.052

Xia, S., Ni, Y., Zhou, Q., & liu, H., Xiang, H., Sui, H., & Shang, D.. (2019). Emodin attenuates severe acute pancreatitis via antioxidant and anti-inflammatory activity. *Inflammation, 42*(6), 2129–2138. https://doi.org/10.1007/s10753-019-01077-z

Zhang, X., Yu, Y., Zhang, J., Qian, X., Li, X., & Sun, X. (2024). Recent Progress regarding Jasmonates in tea plants: Biosynthesis, signaling, and function in stress responses. *International Journal of Molecular Sciences, 25*(2), 1079. https://doi.org/10.3390/ijms25021079